International Journal of Architectural, Civil and Construction Sciences
ISSN: 2415-1734
Vol:6, No:1, 2012

Numerical Modeling of Direct Shear Tests on Sandy Clay

R. Ziaie Moayed , S. Tamassoki , and E. Izadi

***Abstract*—**Investigation of sandy clay behavior is important since urban development demands mean that sandy clay areas are increasingly encountered, especially for transportation infrastructures. This paper presents the results of the finite element analysis of the direct shear test (under three vertical loading 44, 96 and 192 kPa) and discusses the effects of different parameters such as cohesion, friction angle and Young's modulus on the shear strength of sandy clay. The numerical model was calibrated against the experimental results of large-scale direct shear tests. The results have shown that the shear strength was increased with increase in friction angle and cohesion. However, the shear strength was not influenced by raising the friction angle at normal stress of 44 kPa. Also, the effect of different young's modulus factors on stress-strain curve was investigated.

***Keywords*—**Shear strength, Finite element analysis, Large direct shear test, Sandy clay.

I. Introduction

ENGINEERING practice need to predict behavior of engineering structures founded on clay within a certain tolerance, in bridges, road, highway and embankments and cuts. The shear strength is one of the parameters affecting on the behavior of the soils from the geotechnical engineering point of view. The direct shear test is a very popular test for determining shear strength of soils.

Many experimental, analytical, and numerical studies have been performed to investigate the shearing behavior of soils [2]-[4]. The Numerical methods enable the determination of material parameters that would have been difficult to measure in the experimental study [1]-[3]-[6]-[7]-[8]. The development of numerical procedures of calculations caused some important idealizations of the problem. The main ones deal with the following elements: geometry of model; loading conditions; material properties and constitutive models of materials and selection of numerical technique.

The intention of the paper is to show the effects of sandy clay parameters such as cohesion, friction angle and Young's modulus on the shear strength of sandy clay. Numerical calculations were carried out to simulate the material behavior in a direct shear tester [5] and a true simple shear tester under the same initial conditions. In the numerical analysis, a finite element method was used. The material model takes into account the effect of friction angle, Young's modulus and cohesion. The soil parameters were described by the modified Drucker-prager model. The case study investigated here in this study is the one which experimentally studied [9].

R. Ziaie Moayed, Associate Professor, Civil Engineering Department, Imam Khomeini International University (phone: 281-837-1153; fax: 281-837-1153; e-mail: R_ziaie@ikiu.ac.ir).

S. Tamassoki, M.Sc. Student, Civil Engineering Department, Imam Khomeini International University (e-mail: S.tamassoki86@gmail.com).

E. Izadi, M.Sc. Student, Civil Engineering Department, Imam Khomeini International University (e-mail: Ehsanizadi@ikiu.ac.ir).

II. Modified Drucker-Prager model

The Drucker–Prager/cap plasticity model has been widely used in finite element analysis programs for a variety of geotechnical engineering applications. The cap model is appropriate to soil behavior because it is capable of considering the effect of stress history, stress path, dilatancy, and the effect of the intermediate principal stress. The yield surface of the modified Drucker–Prager/cap plasticity model consists of three parts: a Drucker–Prager shear failure surface, an elliptical cap, which intersects the mean effective stress axis at a right angle, and a smooth transition region between the shear failure surface and the cap, as shown in Figure 1. Elastic behavior is modeled as linear elastic using the generalized Hooke's law. Alternatively, an elasticity model in which the bulk elastic stiffness increases as the material undergoes compression can be used to calculate the elastic strains. The onset of plastic behavior is determined by the Drucker–Prager failure surface and the cap yield surface. The Drucker–Prager failure surface is given by:

$$F_s = t - p\tan\beta - d = 0 \quad (1)$$

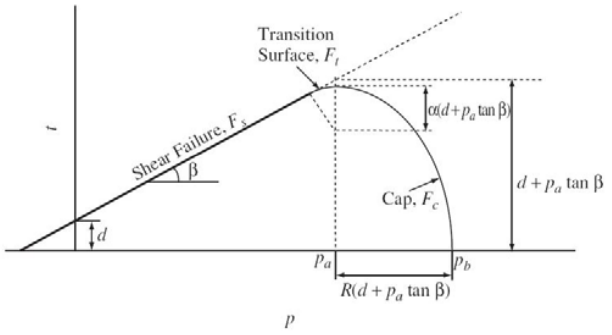

Fig. 1 Yield surfaces of the modified cap model in the p–t plane [10]

Where β is the soil's angle of friction and d is its cohesion in the p–t plane, as indicated in Figure 1. As shown in the figure, the cap yield surface is an ellipse with eccentricity = R in the p–t plane. The cap yield surface is dependent on the third stress invariant, r, in the deviatoric plane as shown in Figure 2

are given by:

$$q = \sqrt{3J_{2D}} = \sqrt{3\left(J_2 - \frac{J_1^2}{6}\right)} = \sqrt{\frac{1}{2}[(\sigma_1-\sigma_2)^2 + (\sigma_2-\sigma_3)^2 + (\sigma_1-\sigma_3)^2]} \quad (2)$$

$$r = \left(\frac{27}{2}J_{3D}\right)^{1/3} = \left(\frac{27}{2}J_3 - 9J_1J_2 + J_1^3\right)^{1/3} \quad (3)$$

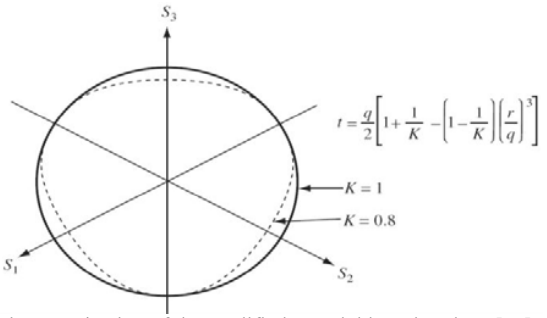

Fig. 2 Projection of the modified cap yield on the-plane [10]

The cap surface hardens (expands) or softens (shrinks) as a function of the volumetric plastic strain. When the stress state causes yielding on the cap, volumetric plastic strain (compaction) results cause the cap to expand (hardening). But when the stress state causes yielding on the Drucker–Prager shear failure surface, volumetric plastic dilation results, causing the cap to shrink (softening). The cap yield surface is given as:

$$F_c = \sqrt{(P - P_a)^2 + \left(\frac{Rt}{1+\alpha-\alpha/cos\beta}\right)^2} - R(d + P_a tan\beta) = 0 \quad (4)$$

Where R is a material parameter that controls the shape of the cap and α is a small number (typically, 0.01 to 0.05) used to define a smooth transition surface between the Drucker–Prager shear failure surface and the cap:

$$F_t = \sqrt{(P - P_a)^2 + [t - (1 - \frac{\alpha}{cos\beta})(d + P_a tan\beta)]^2} - \alpha(d + P_a tan\beta) = 0 \quad (5)$$

P_a is an evolution parameter that controls the hardening–softening behavior as a function of the volumetric plastic strain.

The hardening–softening behavior is simply described by a piecewise linear function relating the mean effective (yield) stress p_b and the volumetric plastic $P_b = P_b(\varepsilon_{vol}^{Pl})$, as shown in Figure 3. This function can easily be obtained from the results of one isotropic consolidation test with several unloading–reloading cycles. Consequently, the evolution parameter, pa, can be calculated as:

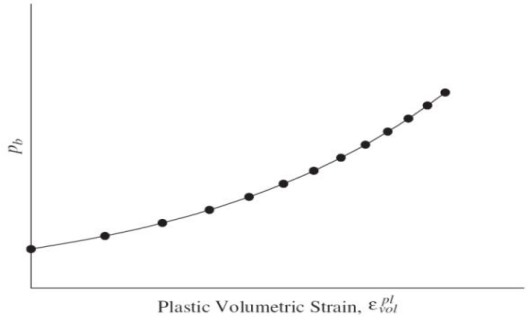

Fig. 3 Typical cap hardening behavior [10]

$$P_a = \frac{P_b - Rd}{1 + Rtan\beta} \quad (6)$$

The Mohr–Coulomb parameters (c ,) can be converted to Drucker–Prager parameters as follows:

$$tan\beta = \frac{6sin\emptyset'}{3 - sin\emptyset'} \quad (7)$$

$$d = \frac{18c\,cos\emptyset'}{3 - sin\emptyset'} \quad (8)$$

The cap hardening curve is obtained from the isotropic consolidation test results (C_c and C_s) then we can calculate the plastic volumetric strain as [10]:

$$\varepsilon_\vartheta^P = \frac{\lambda - \kappa}{1 + e_0} ln\frac{P'}{P_0'} = \frac{C_c - C_s}{2.3(1 + e_0)} ln\frac{P'}{P_0'} \quad (9)$$

In this research, the soils parameters were described by the modified Drucker-Prager plastic model (Cap Plasticity) with an elastic model, using the parameters given in Table I and II. Note that the parameters given in the Table I are taken from previous studies [9].

III. Finite Element Modeling And Analysis

A. Model geometry

A series of 3D finite element analysis has been conducted to simulate the large-scale direct shear tests using ABAQUS 6.9 application. The model geometry is shown in figure 4. The metal box of the direct shear apparatus was modeled by rigid surfaces in the numerical model. The interface between soil and box walls was modeled using Tie constraint by discretization method surface-to-surface capability implemented in ABAQUS/Standard.

TABLE I
GEOTECHNICAL PARAMETERS OF THE STUDIED SOIL [9]

Symbol	Quantity	Value
ρ	Dry unit weight	18.15 kN/m3
c	Cohesion	32 kPa
φ	Friction angle	29.94 [°]
ϑ	Poisson's ratio	0.25
E	Young's modulus for normal stresses 44, 96 and 192 kPa	7, 8 and 8.5 MPa

TABLE II
EQUIVALENT DRUCKER-PRAGER PARAMETERS OF THE STUDIED SOIL

Symbol	Quantity	Value [a]
d	Material Cohesion	200 kPa
β	Angle of Friction	50.13 °
R	Cap Eccentricity	0.2
-	Initial cap yield surface position	-
α	Transition surface radius	0.01
K	Flow Stress Ratio	0.778

B. Loading condition

The analysis was carried out considering two steps. In the first step, only normal stress was applied on the top surface of the model and in the second step, shear stress was applied. All of the analyses were performed using normal stresses of 44, 96, and 192 kPa.

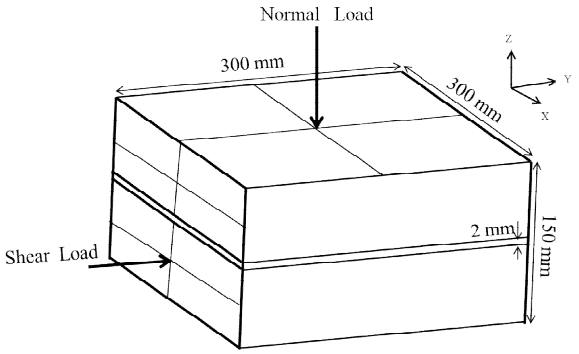

Fig. 4 The model geometry (the dimension of the boxes are according to ASTM-D5321)

C. Boundary condition

Figure 5 shows the boundary condition of the occupied model. The bottom of the model is restrained in x and z direction. In the initial and first step, the upper box is restrained in x, y direction and The lateral walls of upper and beneath boxes are restrained against in movements in x, y and z. In the second step, the lateral walls of upper box are restrained in x, y and z, however the beneath box is restrained in x, z and a horizontal displacement of about 0.01 mm is applied to the beneath box in y direction.

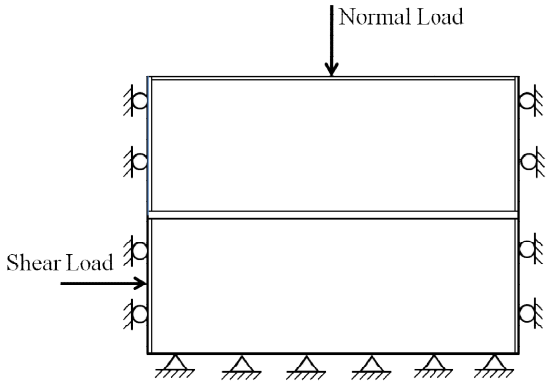

Fig. 5 Boundary conditions of model

The FE mesh of the model is shown in the Figure 6. Because of the composite geometry of the problem, the mesh was implemented using "structured mesh" technique in ABAQUS application. The sandy clay was modelled by C3D8R (8-node linear brick, reduced integration, hourglass control) elements. Dynamic analysis was occupied here in this work.

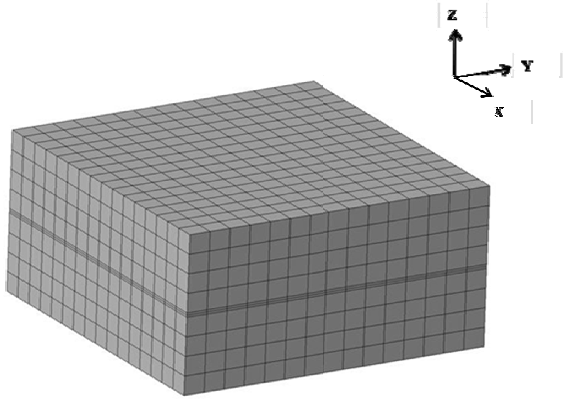

Fig. 6 3D mesh of modeling of direct shear test

IV. RESULTS AND DISCUSSION

The analysis carried out for each three normal stress 44, 96 and 192 kPa in FE model. The results are in a good agreement with experimental data obtained from the case study which mentioned before [9], the results of numerical modeling are shown in Fig. 7.

A. Effect of friction angle

The effect of friction angle on shear strength is illustrated in Figure 8. As shown in this figure, the shear strength of soil was increased with increase in friction angle in normal stress 96 and 192 kPa.

However, the shear strength was not influenced by raising the friction angle at normal stress of 44kPa. In normal stresses of 96 and 192 kPa, an increment in friction angle lead to increase the interlocking between soil particles and hence increasing shear strength of soil.

B. Effect of cohesion

Figure 9 shows the effect of cohesion on shear strength of soil. It is found that an increase in the magnitude of cohesion can raise the shear strength. Table III gives relationship between cohesion and shear strength under different normal stresses.

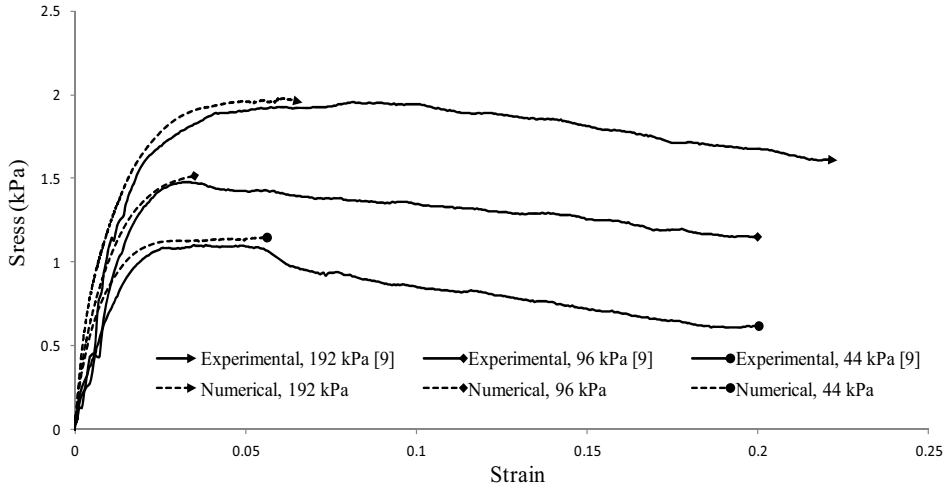

Fig. 7 Comparison of experimental and numerical modeling of direct shear test on sandy clay

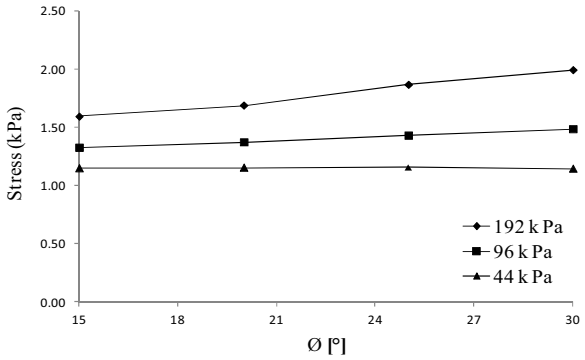

Fig. 8 Effect of friction angle on shear strength of sandy clay

TABLE III
EQUATIONS BETWEEN COHESION AND SHEAR STRENGTH

Normal stress	Equation	R^2
192 kPa	y = 59.723x + 2523.3	0.99
96 kPa	y = 69.94x + 745.72	0.99
44 kPa	y = 70.12x + 342.29	1

x: Index cohesion (kPa).
y: Index shear strength (N).
R^2: coefficient correlation.

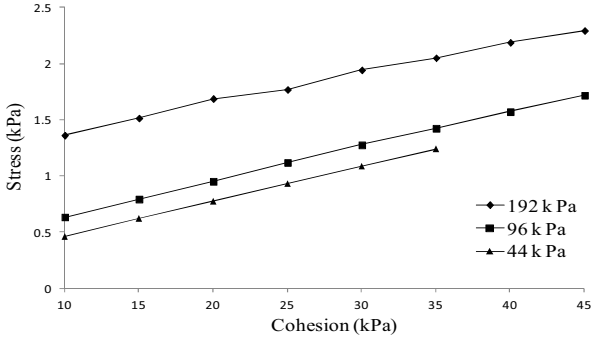

Fig. 9 Effect of cohesion on shear strength of sandy clay

C. Effect of Young's modulus:

The elasticity modulus of soil is not a unique property but varies widely with stress level, stress history, time, type of loading, and soil disturbance. In general, the modulus of a soil decreases with

1. An increase in deviator stress.
2. Soil disturbance.

And it increases with:

1. An increase in consolidation stress.
2. An increase in over consolidation ratio.
3. An increase in aging.
4. An increase in strain rate [11].

Figure 10 shows the effect Young's modulus on stress-strain curve gradient (which is another definition for the stiffness). It is observed that increasing the elasticity modulus lead to increase the shear stiffness of the soil samples.

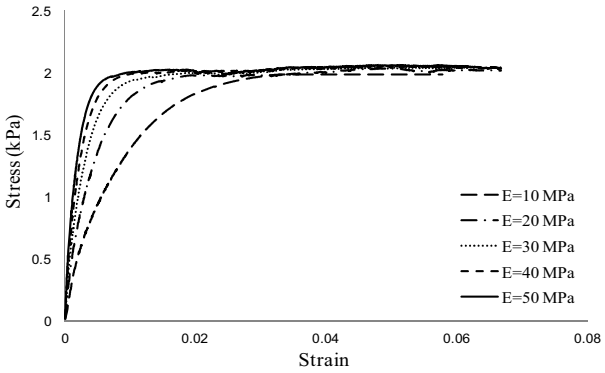

(a) Normal stress of 192 kPa

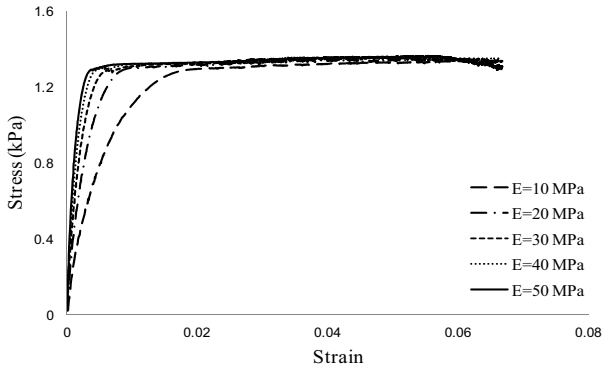

(b) Normal stress of 96 kPa

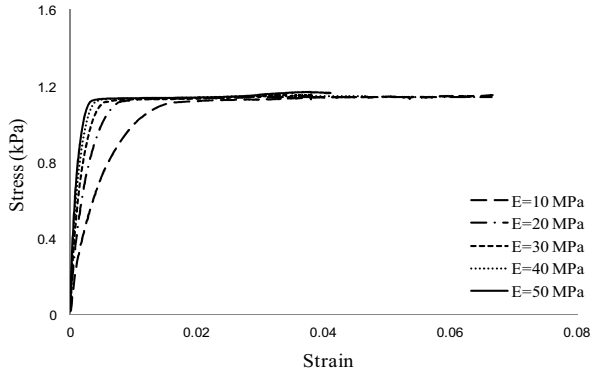

(c) Normal stress of 44 kPa

Fig. 10 Effect of different Young's modulus on the shear strength

V. Conclusion

The present study shows a set of analyses were carried out on sandy clay. The parameters such as cohesion, friction angle and Young's modulus varied in analysis and their effects on shear strength of sandy clay were investigated. The following conclusions could be drawn;

(1) The numerical model was in good agreement with experimental results of large-scale direct shear tests on sandy clay.

(2) The shear strength is not affected by friction angle at normal stress of 44 kPa. However, at normal stresses of 96 and 192 kPa the shear strength is increased.

(3) With increase in cohesion, the magnitude of shear strength was increased.

(4) An increment in Young's modulus leads to increase the stiffness of the soil.

References

[1] A. Iizuka, K. Kawai, , E.R. Kim, and M. Hirata, "Modeling of the confining effect due to the geosynthetic wrapping of compacted soil specimens," *Geotextiles and Geomembranes,* vol. 22, pp. 329–358, 2004.

[2] A. Bagherzadeh-Khalkhali, A. Asghar Mirghasemi, "Numerical and experimental direct shear tests for coarse-grained soils," *Particuology*, vol. 7, pp. 83–91, 2009.

[3] E.M. Palmeira, "Soil–geosynthetic interaction: modelling and analysis," *Geotextiles and Geomembranes 27*, pp. 368–390, 2009.

[4] J. WookPark, J. JoonSong, "Numerical simulation of a direct shear test on a rock joint using a bonded-particlemodel," *International Journal of Rock Mechanics & Mining Sciences*, vol. 46, pp. 1315–1328, 2009.

[5] JG. Potyondy, "Skin friction between various soils and construction materials," *Geotechnique*, vol. 4, pp. 339–353, 1961.

[6] H.J. Burd, G.T. Houlsby, "Numerical modeling of reinforced unpaved roads," *Proceeding of the Third International Symposium on Numerical Models in* Geomechanics, Canada, 1989.

[7] K. Kazimierowicz-Frankowska, "Influence of geosynthetic reinforcement on the load-settlement characteristics of two-layer sub grade," *Geotextiles and Geomembranes* , vol. 25, pp. 366–376, 2007.

[8] P.K. Anubhav, Basudhar, "Modeling of soil–woven geotextile interface behavior from direct shear test results," *Geotextiles and Geomembranes* , vol. 28, pp. 403–408, 2010.

[9] R. Ziaie Moayed, M. Kamalzare, "Influence of Geosynthetic Reinforcement on Shear Strength Characteristics of Two-Layer Sub grade," *Imam Khomeini International University Department of Engineering*, June 2010.

[10] S. Helwany, "Applied Soil Mechanics with ABAQUS Application," *Printed in the United States of America*, pp. 61–66, 2007.

[11] T. William Lambe, R.V. Whitman, "Soil Mechanics," SI Version, Massachustts Institute of Technology With the assistance of H. G. Poulos University of Sydney, 1928.